Viral neuroinvasion and neurotropism without neuronal damage in the hACE2 mouse model of COVID-19

Running title: CNS involvement in SARS-CoV-2 infection of hACE2 mice

Frauke Seehusen[1], Jordan J. Clark[2], Parul Sharma[2], Krishanthi Subramaniam[2], Sabina Wunderlin Giuliani[1], Grant L. Hughes[3], Edward I. Patterson[3], Benedict D. Michael[4], Andrew Owen[4], Julian A. Hiscox[2], James P. Stewart[2], Anja Kipar[1,2]

[1] Laboratory for Animal Model Pathology, Institute of Veterinary Pathology, University of Zurich, Switzerland.
[2] Department of Infection Biology & Microbiomes, Institute of Infection, Veterinary and Ecological Sciences, University of Liverpool, UK.
[3] Departments of Vector Biology and Tropical Disease Biology, Centre for Neglected Tropical Disease, Liverpool School of Tropical Medicine, Liverpool, UK.
[4] Department of Clinical Infection Microbiology and Immunology, Institute of Infection, Veterinary and Ecological Sciences, University of Liverpool, UK.
[5] Department of Pharmacology and Therapeutics, Centre of Excellence in Long-acting Therapeutics (CELT), University of Liverpool, UK.

*Authors' ORCID IDs and Email addresses:
Frauke Seehusen: 0000-0001-6701-7868; frauke.seehusen@uzh.ch
Jordan J Clark: Jordan.Clark@liverpool.ac.uk
Parul Sharma: Parul.Sharma@liverpool.ac.uk
Krishanthi Subramaniam: 0000-0002-1734-9351; K.Subramaniam@liverpool.ac.uk
Sabina Wunderlin Giuliani: sabina.wunderlin@vetpath.uh.ch
Grant L Hughes: grant.hughes@lstmed.ac.uk
Edward I Patterson: ian.patterson@lstmed.ac.uk
Benedict D Michael: 0000-0002-8693-8926; Benedict.Michael@liverpool.ac.uk
Andrew Owen: aowen@liverpool.ac.uk
Julian A Hiscox: Julian.Hiscox@liverpool.ac.uk
James Stewart: 0000-0002-8928-2037; J.P.Stewart@liverpool.ac.uk
Anja Kipar: 0000-0001-7289-3459; anja.kipar@uzh.ch, akipar@liverpool.ac.uk

Corresponding author:
Anja Kipar
Institute of Veterinary Pathology
Vetsuisse Faculty
University of Zurich
Winterthurerstrasse 268
CH - 8057 Zurich
Switzerland

Abstract

Coronavirus disease 2019 (COVID-19) is a primarily respiratory disease with variable clinical courses for which animal models are needed to gather insights into the pathogenesis of its causative virus, Severe Acute Respiratory Syndrome Coronavirus 2 (SARS-CoV-2), in human patients. SARS-CoV-2 not only affects the respiratory tract but also the central nervous system (CNS), leading to neurological symptoms such as loss of smell and taste, headache, fatigue or severe complications like cerebrovascular diseases. Transgenic mice expressing human angiotensin-converting enzyme 2 (hACE2) under the cytokeratin 18 promoter (K18-hACE2) represent a well-known model of SARS-CoV-2 infection. In the present study, it served to investigate the spatiotemporal distribution and pathomorphological features in the CNS following intranasal infection with relatively low SARS-CoV-2 doses and after prior influenza A virus infection.

In K18-hACE2 mice, SARS-CoV-2 was found to frequently spread to and within the CNS during the later phase (day 7) of infection. Infection was restricted to neurons and appeared to first affect the olfactory bulb and spread from there mainly in basally orientated regions in the brain and into the spinal cord, in a dose dependent manner and independent of ACE2 expression. Neuronal infection was not associated with cell death, axonal damage or demyelination. However, microglial activation, microgliosis and a mild macrophage and T cell dominated inflammatory response was consistently observed. This was accompanied by apoptotic death of endothelial, microglial and immune cells, without evidence of viral infection of glial cells, endothelial cells and leukocytes.

Taken together, microgliosis and immune cell apoptosis indicate a potential important role of microglial cells for the pathogenesis and viral effect in COVID-19 and possible impairment of neurological functions, especially in long COVID. These data may also

be informative for the selection of therapeutic candidates, and broadly support investigation of agents with adequate penetration into relevant regions of the CNS.

Keywords: Severe Acute Respiratory Syndrome Coronavirus 2, mouse model, COVID-19, encephalitis, microgliosis, influenza A virus coinfection

Introduction

As of April 2021, the newly emerged betacoronavirus, Severe Acute Respiratory Syndrome Coronavirus-2 (SARS-CoV-2) has infected over 135 million people globally, with over 2.9 million deaths due to the associated disease, COVID-19 (WHO, COVID-19 Weekly Epidemiological Update, 13th April 2021). The majority of COVID-19 patients display respiratory symptoms. However, a proportion of patients develop mostly transient unspecific neurological signs like loss of smell and taste (anosmia, ageusia), headache, or dizziness. Fatal cases can also be associated with ischemic stroke, hemorrhagic encephalopathy and epileptic seizures as well as meningoencephalitis (Bernard-Valnet et al., 2020; Helms et al., 2020a; Huang et al., 2020; Mao et al., 2020; Moriguchi et al., 2020; Oxley et al., 2020; Poyiadji et al., 2020).

There is evidence of viral entry into the brain through the olfactory or vagal nerve and/or the oral and ophthalmic routes, with trans-synaptic neuronal spread to other brain regions (Cantuti-Castelvetri et al., 2020; Matschke et al., 2020; Meinhardt et al., 2021); this could provide a link to the frequently reported (initial) anosmia and ageusia. In addition, hematogenous spread to the brain via infection of endothelial cells and/or immune cells is suspected (Paniz-Mondolfi et al., 2020; Al-Sarraj et al., 2021).

97 Pathomorphological findings reported in the brain of fatal human COVID-19 cases
98 are variable and present as vascular/hemodynamic/ischemic lesions like ischemic
99 infarcts and/or mild inflammatory changes; neuronal or axonal damage and acute
100 disseminated encephalomyelitis have been reported in rare cases (Deigendesch et
101 al., 2020; Fabbri et al., 2021; Jaunmuktane et al., 2020; Kantonen et al., 2020;
102 Matschke et al, 2020; Schurink et al., 2020; Solomon et al., 2020; Reichard et al.,
103 2020; von Weyhern et al., 2020). Focal or diffuse microglial activation or microglial
104 nodules have also been observed (Al-Dalahmah et al., 2020; Bussani et al., 2020;
105 Deigendesch et al., 2020; Jaunmuktane et al., 2020; Matschke et al., 2020; Schurink
106 et al., 2020; Fabbri et al., 2021). COVID-19 patients can harbor SARS-CoV-2 RNA
107 and protein in the brain (Matschke et al., 2020; Puelles et al., 2020; Meinhardt et al.,
108 2021), and a recent study using human brain organoids provided strong evidence
109 that SARS-CoV-2 replicates in neurons (Song et al., 2021). However, presence of the
110 virus was not found to be associated with the severity of neuropathological changes
111 (Matschke et al., 2020), and in a recent study, immunohistochemical staining for
112 SARS-CoV-2 failed to detect viral antigen in all 18 investigated patients, while low
113 levels of viral RNA were detected by RT-PCR in five patients (Solomon et al., 2020).
114 Encephalopathy, as a severe complication in COVID-19, is often associated with
115 systemic hyperinflammation mainly provoked by an aberrantly excessive innate
116 immune response (Najjar et al. 2020). It is suspected that not only a direct virus
117 induced endotheliitis, but also a maladaptive innate immune response may impair
118 neurovascular endothelial function and cause disruption of the blood-brain barrier
119 (BBB), activation of innate immune signalling pathways and a parainfectious
120 autoimmunity (Najjar et al., 2020).
121 Recent articles have discussed the role of glial cells in COVID-19
122 encephalopathies (Murta et al., 2020; Vargas et al., 2020). Glial cells might not only

123 represent potential targets for viral infection but are also highly sensitive to systemic
124 proinflammatory cytokines (Perry et al., 2007; Teeling and Perry, 2009; Murta et al.,
125 2015; Murta and Ferrari, 2016). In COVID-19 patients, the massive systemic release
126 of inflammatory cytokines could affect endothelial cells and astrocytes of the BBB,
127 thus facilitating viral entry like in other viral brain diseases such as HIV-1 encephalitis
128 and measles (Swanson and McGavern, 2015). Indeed, a recent study has shown that
129 SARS-CoV-2 spike protein S1 from the blood can pass the BBB and thereby gain
130 access to the brain parenchyma in mice, potentially triggering a parenchymal
131 response without the presence of intact virus (Rhea et al., 2021). Furthermore,
132 astrocytes and microglia may contribute to the local neuroinflammatory response of
133 the CNS (Michael et al., 2020; Murta et al., 2020). Also, microglial cells are
134 hypothesized to be involved in the innate immune response and facilitate viral
135 clearance, recruitment of immune cells as well as activation of antiviral responses
136 and cytokine production in the brain of COVID-19 patients (Vargas et al., 2020).
137 Some authors also propose that a SARS-CoV-2-induced proinflammatory microglial
138 phenotype might contribute to the development of subsequent neurodegenerative
139 disorders (Alam et al., 2020; Mahalaxmi et al., 2020). Furthermore, the
140 proinflammatory priming of microglia, either by direct SARS-CoV-2 infection or a
141 peripheral cytokine storm, could exacerbate disease, as indicated in experimental
142 murine coronavirus (MHV-A59) infection (Lavi and Cong, 2020).
143 The human angiotensin-converting enzyme 2 (hACE2) is considered to be the
144 main host receptor for SARS-CoV-2, binding to the viral spike protein (S) (Hoffmann
145 et al., 2020). The K18-hACE2 transgenic (K18-hACE2) mouse, where hACE2
146 expression is driven by the epithelial cell cytokeratin-18 (K18) promoter, was
147 developed to study the pathogenesis of SARS-CoV infection (McCray et al., 2007); it
148 is now frequently employed to address a broad range of questions regarding SARS-

149 CoV-2 as expression of human ACE2 (hACE2) appears to convey higher binding
150 affinity than its murine counterpart. Several recent studies have shown that intranasal
151 SARS-CoV-2 infection of K18-hACE2 mice reaches the brain where it spreads
152 widely. Infection of the brain can be associated with non-suppurative
153 (meningo)encephalitis (Carossino et al., 2021; Clark et al., 2021; Kumari et al, 2021;
154 Song et al., 2021). With high infectious doses (10^5 PFU), very high viral loads were
155 found in the brain at a time when lung burdens had already decreased, in association
156 with upregulation of IFN-α as well as proinflammatory cytokine and chemokine
157 transcription; the authors posited that lethal outcome of infection in these mice was a
158 consequence of neuroinvasion (Kumari et al, 2021). Another study using an even
159 higher viral inoculum (10^6 PFU) elicited CNS signs (tremors, proprioceptive defects,
160 abnormal gait, imbalance) by day 6/7 after infection (Carossino et al., 2021). Studies
161 in mice have also confirmed that the virus can get access to the brain via the
162 olfactory bulb (Rhea et al., 2020; Song et al., 2021).
163 Detailed information on the effect of SARS-CoV-2 in the brain of COVID-19
164 patients has so far been collected from fatal cases. However, there is a current
165 paucity of data relating to what happens in the brain of patients that do not have
166 severe disease, recover from it or develop long COVID-19. A better understanding of
167 the viral dynamics within the CNS will provide further insight into the disease
168 pathology and will be highly informative for therapeutics development by providing
169 insight into the prerequisites for distribution of new medicines in development. The
170 present study represents a first attempt to address this question by investigating the
171 CNS of K18-hACE2 mice after intranasal infection with a low to moderate dose of a
172 SARS-CoV-2 wildtype strain, also in combination with prior influenza A virus infection
173 as it seems to foster neuronal spread (Clark et al., 2021).
174

175

176 **Material and Methods**

177 *Cell culture and virus*

178 A PANGO lineage B strain of strain of SARS-CoV-2 (hCoV-
179 2/human/Liverpool/REMRQ0001/2020) cultured from a nasopharyngeal swab from a
180 patient, was passaged in Vero E6 cells (Patterson et al., 2020). The fourth virus
181 passage (P4) was used for infections after it had been checked for deletions in the
182 mapped reads and the stock confirmed to not contain any deletions that can occur on
183 passage (Clark et al., 2021).

184 Influenza virus A/HKx31 (X31, H3N2) was propagated in the allantoic cavity of 9-
185 day-old embryonated chicken eggs at 35 °C. Titres were determined by an influenza
186 plaque assay using MDCK cells (Clark et al., 2021).

187

188 *Biosafety*

189 All work was performed in accordance with risk assessments and standard operating
190 procedures approved by the University of Liverpool Biohazards Sub-Committee and
191 by the UK Health and Safety Executive. Work with SARS-CoV-2 was performed at
192 containment level 3 by personnel equipped with respirator airstream units with filtered
193 air supply.

194

195 *Animals and virus infections*

196 Animal work was approved by the local University of Liverpool Animal Welfare and
197 Ethical Review Body and performed under UK Home Office Project Licence
198 PP4715265. Mice carrying the human ACE2 gene under the control of the keratin 18
199 promoter (K18-hACE2; formally B6.Cg-Tg(K18-ACE2)2Prlmn/J) were purchased

200 from Jackson Laboratories. Mice were maintained under SPF barrier conditions in
201 individually ventilated cages.
202 Animals were randomly assigned into multiple cohorts. For SARS-CoV-2 infection,
203 mice were anaesthetized lightly with isoflurane and inoculated intra-nasally with 50 µl
204 containing 10^3 PFU (cohorts 1 and 2) or 10^4 PFU (cohort 3) SARS-CoV-2 in PBS;
205 control animals received PBS. For double infections (cohort 2), mice were first
206 infected with IAV; they were anaesthetized lightly with KETASET i.m. and inoculated
207 intranasally with 10^2 PFU IAV X31 in 50 µl sterile PBS. Three days later, they were
208 infected with SARS-CoV-2, as described above. Mock-infected mice served as
209 controls. Mice were monitored for any clinical signs and weighed. Animals were
210 sacrificed at 3 or 7 days post SARS-CoV-2 infection by an overdose of
211 pentabarbitone. Tissues were removed immediately for downstream processing; the
212 lungs were processed for another study (Clark et al., 2021).
213
214 *Tissue collection, preparation and processing*
215 For the present study, the heads and spinal cords (C1-T12) were collected and fixed
216 in 10% neutral buffered formal saline for 24-48 h. Brains were exenterated and
217 coronal sections prepared. Heads were sawn longitudinally in the midline for
218 histological assessment of the nasal cavity, cribriform plate and rostral parts of the
219 olfactory bulb that had not been removed with the brain. In cases where SARS-CoV-
220 2 viral antigen was detected in the brain (see below), the spinal cords were sawn into
221 appr. 1.5 mm thick cross sections, using a diamond saw (Exakt 300; Exakt). Heads
222 and spinal cord were gently decalcified in RDF (Biosystems) for twice 5 days, at room
223 temperature (RT) and on a shaker. Brains, heads and spinal cords were routinely
224 paraffin wax embedded.
225

226 *Histology, immunohistology*

227 Consecutive sections (3-5 µm) were either stained with hematoxylin and eosin (HE)
228 or used for immunohistochemistry (IH). IH was performed using the horseradish
229 peroxidase (HRP) method to detect viral antigens in all examined tissues in all
230 animals, and to identify macrophages/activated microglial cells (Iba1+), T cells
231 (CD3+), B cells (CD45R/B220+) and neutrophils (Ly6G+) and to highlight astrocytes
232 (glial fibrillary acidic protein, GFAP+), apoptotic cells (cleaved caspase 3+),
233 disturbances of the fast axonal transport indicating acutely damaged neuronal axons
234 (amyloid precursor protein, APP+) and ACE2 expression in those animals where viral
235 antigen was detected in the brains. Antibodies and detection systems are listed in
236 Supplemental Table S1. Briefly, after deparaffination, sections underwent antigen
237 retrieval in citrate buffer (pH 6.0) or Tris/EDTA buffer (pH 9) for 20 min at 98 °C,
238 followed by incubation with the primary antibodies (diluted in dilution buffer, Agilent
239 Dako). This was followed by blocking of endogenous peroxidase (peroxidase block,
240 Agilent Dako) for 10 min at RT and incubation with the appropriate secondary
241 antibodies/detection systems, all in an autostainer (Dako Agilent or Ventana).
242 Sections were subsequently counterstained with hematoxylin.

243 The brain of a mock-infected control hACE mouse served as normal brain control
244 for ACE2, GFAP and APP, and a lymph node from a normal mouse for the leukocyte
245 and apoptosis markers. Sections from the lungs served as internal positive controls
246 for SARS-CoV-2 and IAV antigen expression, and sections incubated without the
247 primary antibodies served as negative controls.

248

249 *RNA in situ hybridization (RNA-ISH)*

250 RNA ISH was performed using the RNAscope® ISH method (Advanced Cell
251 Diagnostics (ACD Advanced Cell Diagnostics, Newark, California) and the

252 RNAscope® 2.5 Detection Reagent Kit (Brown) according to the manufacturer's
253 protocol and as previously described (Salguero et al., 2021; Saura-Martinez et al.,
254 2021). All cases were first tested for the suitability of the tissue (RNA preservation
255 and quality) with an oligoprobe for *Mus musculus* peptidylprolyl isomerase B (PPIB)
256 mRNA (ACD). Those yielding good PPIB signals were then subjected to RNA-ISH for
257 nCoV2019-S (coding for Wuhan seafood market pneumonia virus isolate Wuhan-Hu-
258 1 complete genome; Genbank NC_045512.2). Briefly, sections were heated to 60 °C
259 for 1 h and subsequently deparaffinized. Permeabilization was achieved by
260 incubating the section in pretreatment solution 1 (RNAscope® Hydrogen Peroxide) for
261 10 min at RT, followed by boiling in RNAscope® 1X Target Retrieval Reagents
262 solution at 100 °C for 15 min and washing in distilled water and ethanol. After
263 digestion with RNAscope® Protease Plus for 30 min at 40 °C, sections were
264 hybridized with the oligoprobes at 40 °C in a humidity control tray for 2 h (HybEZ™
265 Oven, ACD). Thereafter a serial amplification with different amplifying solutions
266 (AMP1, AMP2, AMP3, AMP4: alternating 15 min and 30 min at 40 °C) was
267 performed. Between each incubation step, slides were washed with washing buffer.
268 They were subsequently incubated with AMP 5, AMP 6 and DAB at RT for 30 and 15
269 min respectively. Gill's hematoxylin served to counterstain the sections which were
270 then dehydrated with graded alcohol and xylene and coverslipped. A lung section
271 from an infected mouse at 3 dpi served as a positive control. The negative control
272 was consecutive sections incubated accordingly but without including the
273 hybridization step.
274
275

276 **Results**

277 *In K18-hACE2 mice, the later phase of SARS-CoV-2 infection is accompanied by*
278 *virus spread into the central nervous system*

279 To assess whether SARS-CoV-2 gains access to the CNS after intranasal infection
280 with a low to medium viral dose we examined groups of K18-hACE2 mice that had
281 been infected with a clinical isolate of SARS-CoV-2 (strain hCoV-
282 19/England/Liverpool_REMRQ0001/2020), at 10^3 and 10^4 PFU, respectively. In
283 addition, we examined mice that had been infected with the lower viral inoculum at
284 day 3 post intranasal infection with 10^2 PFU IAV (strain A/X31). SARS-CoV-2
285 infected mice began to lose weight at 4 dpi and continued to lose weight until the end
286 of the experiment, at 7 dpi. In the sequential IAV then SARS-CoV-2 infected mice,
287 the weight loss was accelerated leading to more rapid and higher mortality, as
288 determined by a humane endpoint of 20% weight loss (Clark et al., 2021).

289 At day 3 post intranasal SARS-CoV-2 infection with 10^3 PFU, viral antigen was
290 detected in numerous individual and aggregates of occasionally degenerate epithelial
291 cells in the nasal cavity in all 4 single SARS-CoV-2 infected animals and in 2 of the 4
292 double infected animals. Viral antigen was also found in the lungs, in both type I and
293 II pneumocytes and, occasionally, capillary endothelial cells, in randomly distributed
294 and variably sized patches of alveoli, with only occasional degenerate cells. This was
295 associated with a mild increase in interstitial cellularity, endothelial cell activation with
296 rolling, emigration and perivascular aggregation of some lymphocytes, and small
297 macrophage aggregates, all as previously reported by this group (Clark et al., 2021).
298 In dual infections, identical SARS-CoV-2 associated lesions were present within
299 areas unaffected by IAV lesions. At this stage, viral antigen was detected in the
300 olfactory epithelium in one animal, but not in brain nerves and brain including

301 olfactory bulb. In dual infected animals, IAV antigen expression was not detected in
302 these structures either, and there were no histological changes.
303 At day 7 post infection, infection of the nasal epithelium was limited; SARS-CoV-2
304 antigen was detected in only rare nasal epithelial cells in most mice, some were
305 negative. As reported (Clark et al., 2021), the lungs of both single and dual infected
306 mice showed multifocal type II pneumocyte activation and syncytial cell formation,
307 with mild mononuclear infiltration, and mild to moderate lymphocyte-dominated
308 vasculitis and perivascular infiltration. There were also a few focal areas of mild
309 desquamative pneumonia with intra-alveolar macrophages/type II pneumocytes,
310 edema and fibrin. Viral antigen expression was restricted to type I and II
311 pneumocytes of unaltered appearing alveoli (data not shown). At this stage, viral
312 antigen was detected in the brain of 2 of the 4 mice that had been infected with the
313 lower dose of SARS-CoV-2 (10^3 PFU) alone, three of the four double infected mice,
314 and all mice that had received the single higher dose (10^4 PFU) of SARS-CoV-2. IAV
315 antigen was not detected in the brain of double infected animals. SARS-CoV-2
316 antigen expression in the brain was associated with its detection in the main olfactory
317 epithelium and the olfactory bulb (Fig. 1A) in all but two animals.
318
319 *In K18-hACE2 mice, SARS-CoV-2 infection in the central nervous system is*
320 *restricted to neurons and spreads in the brain and into the spinal cord in a dose*
321 *dependent manner*
322 In the present study, all animals that were found to harbor viral antigen in the brain
323 showed widespread neuronal expression, but in a dose-dependent manner. In the
324 low dose (10^3 PFU) single infected animals, we only observed individual positive
325 neurons in the olfactory bulb, but no reaction in cranial nerves or the inner ear. In
326 contrast, in both the higher dose (10^4 PFU) single infected and the double infected

327 animals, we found numerous positive neurons in the olfactory bulb (individual
328 cells/neuronal processes in olfactory nerve layer, glomerular layer, almost all cells in
329 external plexiform layer, individual cells in mitral cell layer), and sometimes also
330 aggregates of positive sensory neuronal cells and their dendrites in the olfactory
331 epithelium layer of the main olfactory epithelium (MOE; Fig. 1A). Again, no reaction
332 was seen in cranial nerves.

333 In the brain, viral antigen was detected in a widespread manner across most brain
334 regions in all animals (Fig. 1B), with less extensive viral antigen expression in the low
335 dose single infected animals. Positive neurons were found among others in anterior
336 olfactory nucleus, primary and secondary motor area, primary somatosensory area,
337 anterior cingulate area, gustatory area, auditory area, infralimbic area, lateral and
338 medial septal nucleus, caudoputamen, piriform area, visual area, ectorhinal area,
339 entorhinal area, retrosplenial area, hippocampus and dentate gyrus, subiculum,
340 nearly all midbrain nuclei, thalamus/hypothalamus, amygdalar nuclei, nucleus
341 accumbens, several cranial nerve nuclei (trigeminal, vestibular, hypoglossal nuclei),
342 reticular nucleus, cuneate nucleus, dentate nucleus. These areas are depicted in a
343 3D reference atlas of the Allen Mouse Brain Common Coordinate Framework (Wang
344 et al., 2020; open access) in the following link: https://connectivity.brain-map.org/3d-
345 viewer?v=1&types=PLY&PLY=453%2C1057%2C31%2C44%2C254%2C500%2C92
346 2%2C895%2C549%2C1097%2C386%2C370%2C1132%2C987%2C669%2C1089%
347 2C672%2C502%2C909%2C961%2C972%2C507. Viral antigen expression was
348 most intense in the midbrain. The cerebellum showed only individual or small groups
349 of SARS-CoV-2 positive neurons in a few individual animals (Fig. 1C).

350 In the IAV and SARS-CoV-2 double infected animals as well as in the higher dose
351 single infected animals, the virus had spread to the spinal cord where it was found in
352 neurons in the grey matter (motor neurons and sensory neurons; Fig. 1D, E),

353 stretching through the entire cervical and thoracic spinal cord, or decreasing
354 progressively from the cervical spinal cord.
355 RNA-ISH yielded similar results as immunohistology (Fig. 1C), confirming
356 widespread neuronal infection accentuated in the midbrain.
357

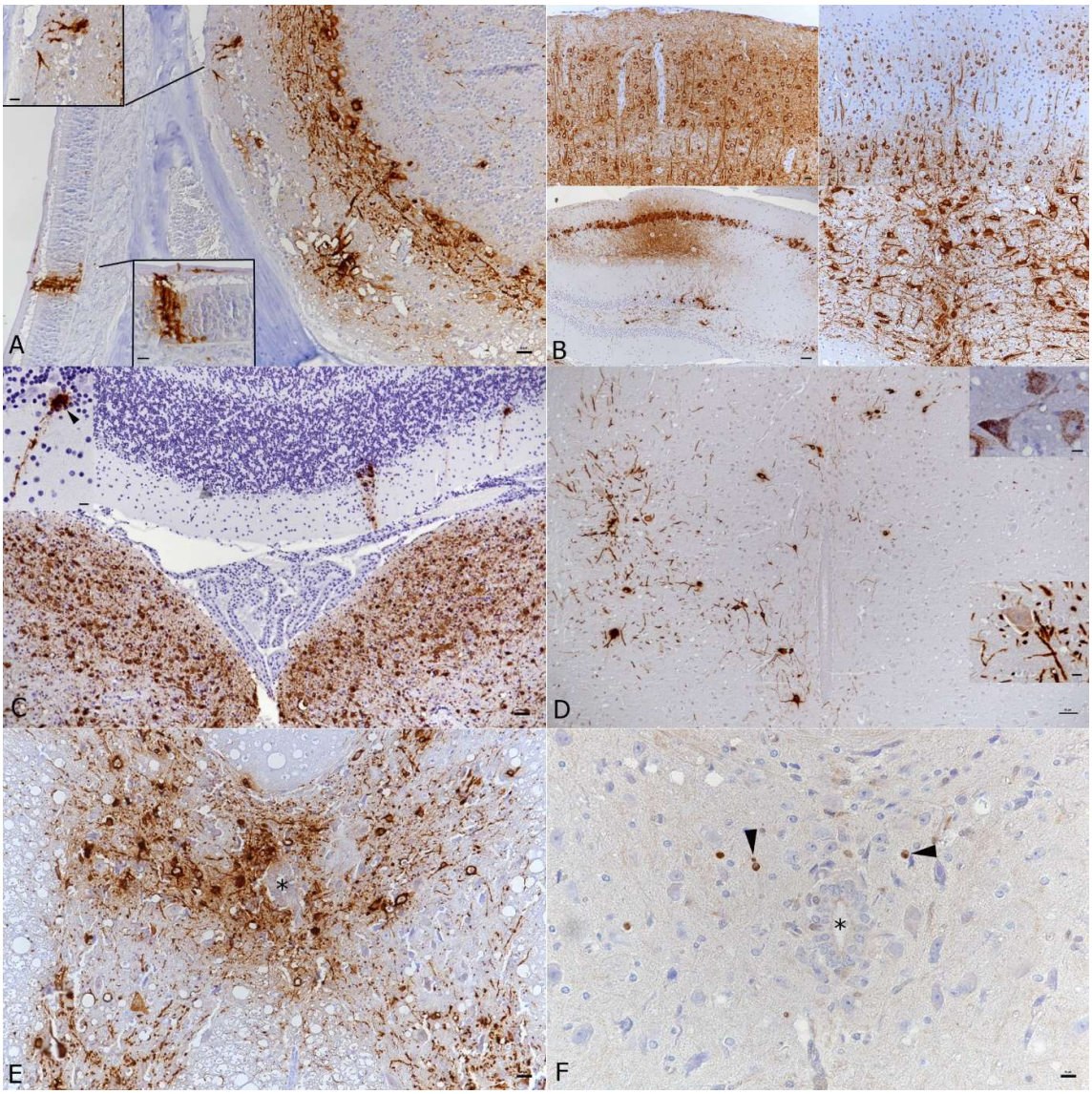

358

359 **Figure 1**. Brain and spinal cord, K18-hACE mice, day 7 post intranasal SARS-CoV-2
360 infection (10^4 PFU as single infection or 10^3 PFU after initial infection with IAV (10^2
361 PFU IAV strain A/X31) as double infection). **A)** Double infected animal, main olfactory
362 epithelium (MOI), cribriform plate and olfactory bulb. Viral antigen is detected in
363 olfactory neurons and basal cells of the MOI and in granule layer, inner and outer
364 plexiform layer, mitral layer as well as glomerular layer of the olfactory bulb. Bar = 20
365 µm. **B)** Double infected animal, examples of viral antigen expression in different
366 brain regions. Top: frontal cortex with viral antigen expression in almost all neurons

367 (left) and mid cortex with proportion of positive neurons (right); bar = 20 µm. Bottom:
368 patchy virus antigen expression in the hippocampus (CA1 and CA3; left; bar = 50
369 µm.) and strong expression in the medulla oblongata (right; bar = 20 µm.). **C)** Single
370 infected animal, medulla oblongata and cerebellum. Viral RNA is abundantly
371 expressed in neurons in the medulla oblongata (vestibular nuclei). The cerebellar
372 cortex exhibits a few positive Purkinje cells (see also inset). Bar = 50 µm. **D)** Single
373 infected animal, thoracic spinal cord. The grey matter exhibits numerous neurons that
374 express viral antigen (large image and bottom inset) and viral RNA (top inset) in cell
375 body and processes. Bar = 50 µm. **E, F)** Double infected animal, thoracic spinal cord.
376 There is extensive viral antigen expression in neurons in the grey matter (E).
377 Consecutive section showing scattered apoptotic (cleaved caspase 3 positive) glial
378 cells (F, arrowheads), among intact neurons and in the absence of an inflammatory
379 reaction. * - central canal. Bars = 20 µm. Immunohistochemistry and RNA-ISH,
380 hematoxylin counterstain.
381

382 *SARS-CoV-2 infection of the brain is associated with diffuse microglial activation and*

383 *a mild macrophage and T cell dominated inflammatory response*

384 In all animals where virus was detected in neurons in the brain, this was associated

385 with a mild nonsuppurative (meningo)encephalitis. The inflammation was only

386 present in areas with SARS-CoV-2-infected neurons. Therefore, it was most

387 pronounced in frontal coronary sections of caudoputamen and the

388 thalamus/hypothalamus region as well as in the hippocampal area and was

389 represented by infiltration of the wall and the perivascular space of small veins by

390 predominantly mononuclear cells, accompanied by a mild increase in parenchymal

391 cellularity (Fig. 2A). The majority of cells in the (peri)vascular infiltrates were Iba1-

392 positive macrophages (Fig. 2B). These were accompanied by T cells (CD3+) which

393 comprised up to approximately 30% of the perivascular cells (Fig. 2C). Individual T

394 cells were also found in the neuroparenchyma, mostly in proximity to perivascular

395 infiltrates (Fig. 2C). The vascular infiltrates contained rare individual neutrophils

396 (Ly6G+) and B cells (CD45R/B220+) (Fig. 2D). The inflammatory infiltrates were

397 accompanied by moderate diffuse microglial activation/microgliosis in areas with

398 SARS-CoV-2 infected neurons (Figs. 2B, E and 3A, B). Microglial nodules were

399 detected mainly adjacent to areas with perivascular infiltrates (Fig. 2E).

The double infected animals also showed a mild lympho-histiocytic meningitis (Clark et al., 2021), more pronounced in caudoputamen, thalamic and hypothalamic regions compared to single infected animals.

There was no evidence of prominent astrogliosis (Fig. 2F). However, astrocytes immediately adjacent to perivascular infiltrates showed hypertrophy of the cytoplasm consistent with activation.

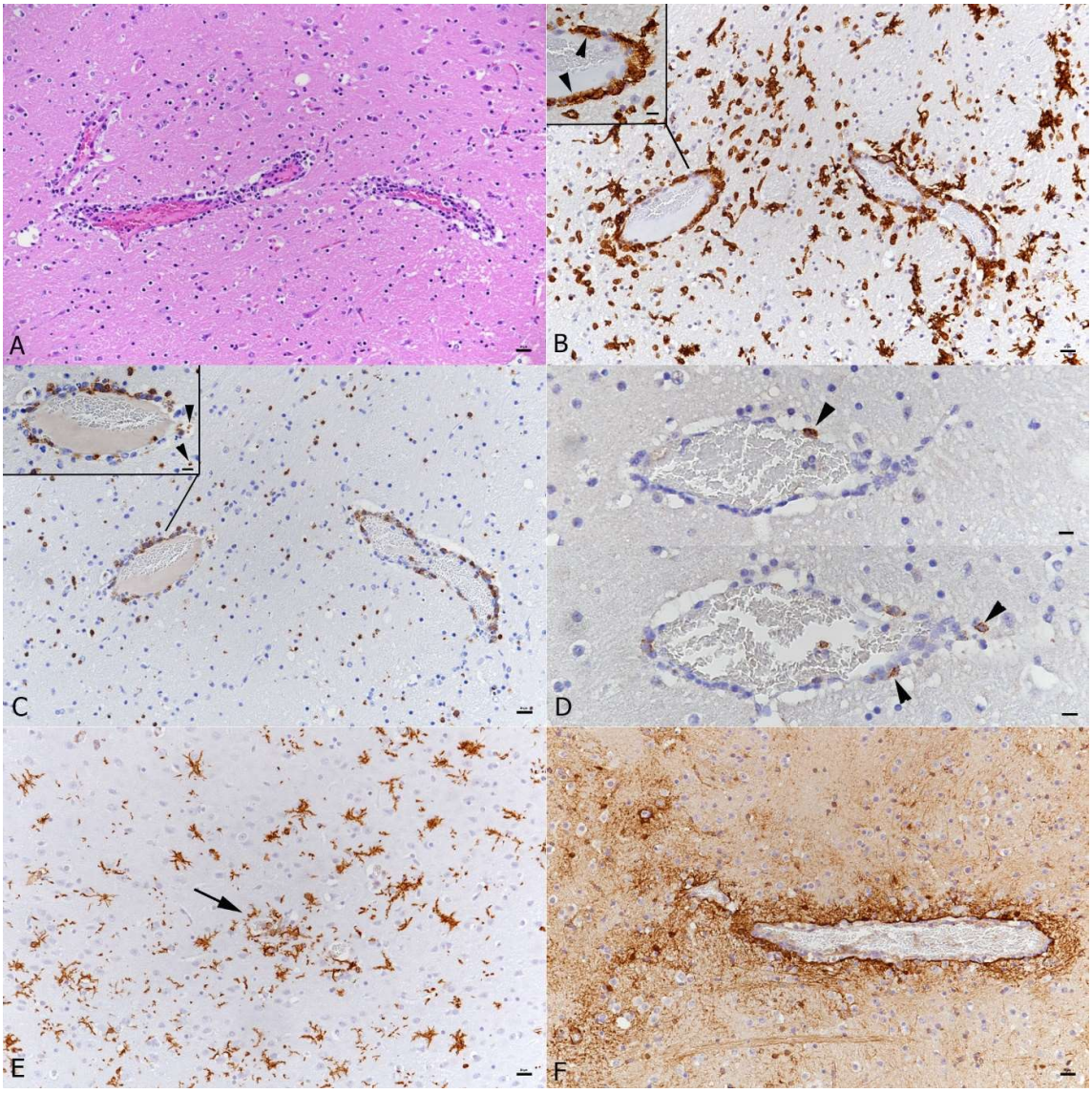

Figure 2. Brain, K18-hACE mouse, day 7 post intranasal SARS-CoV-2 infection (10^4 PFU) after initial infection with IAV (10^2 PFU IAV strain A/X31). **A)** Brain stem with moderate (peri)vascular leukocyte infiltration and mildly increased cellularity in the parenchyma. HE stain. **B)** Macrophages (Iba1+) dominate in the (peri)vascular

412 infiltrate (inset: arrowheads) and the surrounding parenchyma exhibits microglial
413 activation (Iba1+ stellate shaped cells). **C)** T cells (CD3+) are also abundant in the
414 (peri)vascular infiltrates and are found infiltrating the adjacent parenchyma. Inset:
415 vessel with infiltrating T cells; some are degenerate (arrowheads). **D)** Neutrophils
416 (Ly6G+; top, arrowhead) and B cells (CD45R/B220+; bottom, arrowheads) are very
417 rare in the infiltrates. **E.** Brain stem with activated microglial cells (Iba1+) and small
418 microglial nodule (arrow). **F.** Staining of astrocytes (GFAP+) shows hypertrophied
419 astrocytes around a vessel with a mild perivascular infiltrate. B-F:
420 immunohistochemistry, hematoxylin counterstain. Bars = 20 µm.
421

422 *There is no evidence of viral infection of glial cells, endothelial cells or leukocytes or*
423 *of neuronal cell death, axonal damage or demyelination in association with SARS-*
424 *CoV-2 infection, but of apoptotic death of endothelial cells and immune cells*

425 Despite widespread infection of neurons, there was no morphological evidence of
426 neuronal cell death. Staining for cleaved caspase 3 did not mark any neurons. Also,
427 staining for amyloid precursor protein (APP) to detect disturbances in fast axonal
428 transport as an indicator of acute axonal damage did not show any evidence of the
429 latter. Furthermore, there were no changes indicating demyelination of the white
430 matter. Capillary endothelial cells which are positive for ACE2 throughout the brain
431 and spinal cord (Fig. 3C) were negative in both SARS-CoV-2 IHC and ISH. However,
432 in some vessels that exhibited a leukocyte infiltrate, the endothelial layer appeared
433 focally discontinuous (Fig. 3D), confirming vasculitis. The infiltrate contained
434 scattered degenerate cells suggesting a leukocytoclastic component. (Fig. 3D, E).
435 This was confirmed by staining for cleaved caspase 3; both endothelial cells and
436 leukocytes in the vascular infiltrates were found to be apoptotic. Apoptosis (cleaved
437 caspase 3+) was also observed in a few leukocytes (morphology consistent with
438 lymphocytes) in the adjacent parenchyma (likely infiltrating T cells) (Fig. 3E) and in
439 occasional microglial cells (Fig. 3F). In none of the brains was there any evidence of
440 SARS-CoV-2 antigen or RNA expression in glial cells.
441

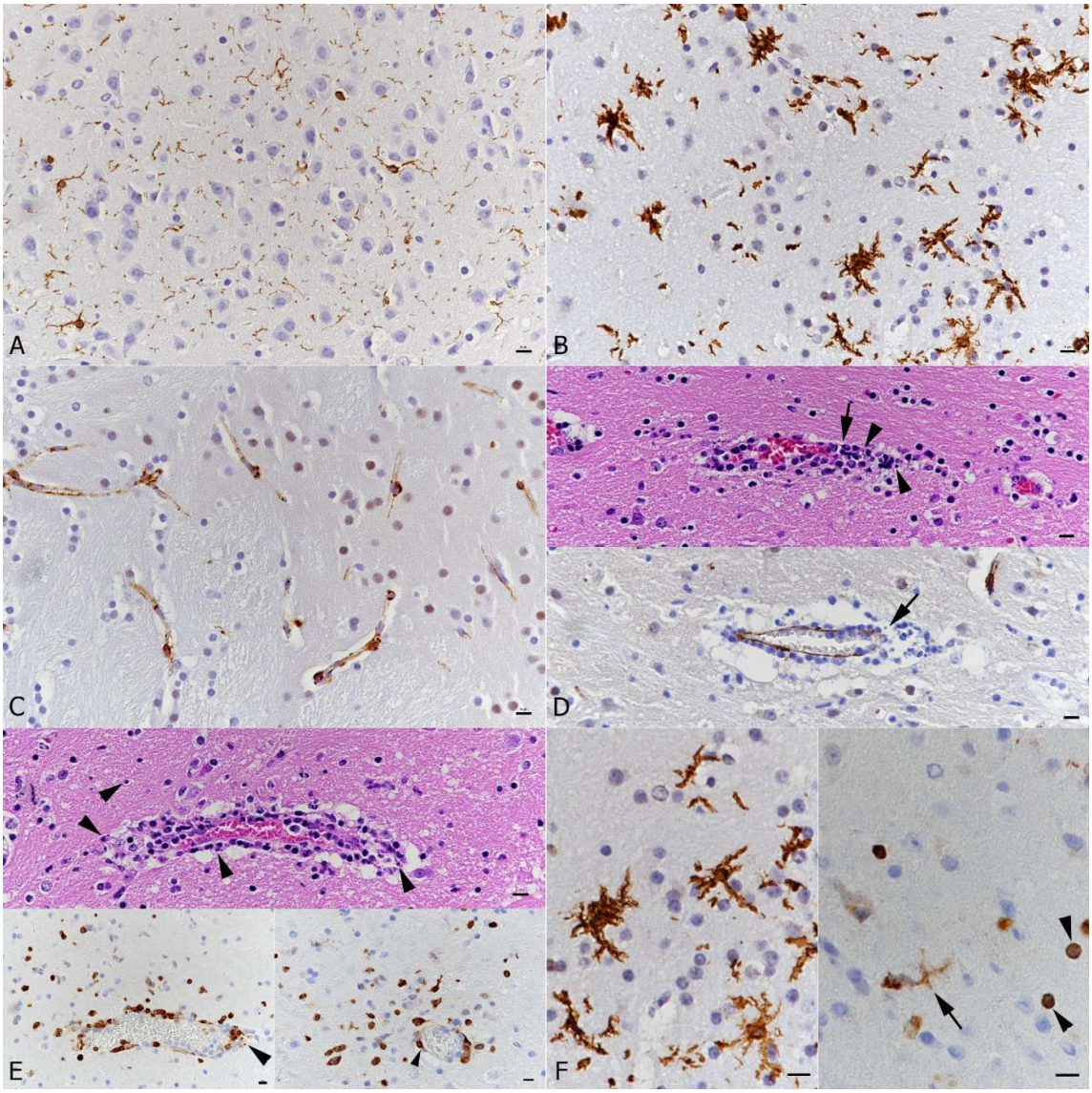

Figure 3. Brain, K18-hACE mice, mock infected and at day 7 post intranasal SARS-CoV-2 infection (10^3 PFU) after initial infection with IAV (10^2 PFU IAV strain A/X31). **A)** Mock infected mouse. Quiescent microglia (Iba1+). **B)** Infected animal. Diffuse microglial activation (Iba1+ stellate cells). **C)** Mock infected mouse. Endothelial cells show cytoplasmic ACE2 expression. **D-F)** Infected animal. **D)** Vessel with moderate leukocyte infiltration with focal destruction of the vessel wall (arrows) and some degenerate leukocytes (leukocytoclastic component). Top: HE stain; bottom: staining for ACE2, showing disruption of the endothelial cells layer. **E)** Vessel with moderate leukocyte infiltration (top: HE stain; bottom: staining for cleaved caspase 3). Individual cells in the infiltrate and in the adjacent parenchyma (top and bottom left: arrowheads) and endothelial cells in an affected vessel (bottom right: arrowhead) undergo apoptosis. **F)** Activated microglia (Iba1+; left). Staining for cleaved caspase 3 (right) shows apoptosis of a microglial cell (arrow) and of small round cells (arrowheads; morphology consistent with lymphocytes). A-E: bars =20 µm; F: bars = 10 µm.

459 **Discussion**

460 COVID-19 is primarily a respiratory disease, with potentially fatal systemic
461 complications that can also involve the CNS. At present, the pathogenetic and clinical
462 role of encephalopathy in COVID-19 patients is controversely discussed. A variety of
463 mild and/or severe clincal signs have been described, and the reported
464 morphological findings in the brain differ between studies; similarly, the presence and
465 distribution of viral RNA or antigen appears to be inconsistent. Many questions are
466 currently still open regarding the infectious route and spatio-temporal distribution of
467 SARS-CoV-2 in the CNS of COVID-19 patients without comorbitidies, showing the
468 need for appropriate animal models.

469 In this context, the hACE2 transgenic mouse under the control of the human
470 cytokeratin 18 promoter, a commonly used mouse model to study pathogenetic
471 effects of SARS-CoV-2 infection, has been employed not only in the present, but also
472 in several other recent studies using the USA-WA1 strain, predominantly at high
473 doses (10^5 to 1.5 x 10^6 PFU) (Oladunni et al., 2020; Carossino et al., 2021; Kumari et
474 al., 2021, Song et al., 2021; Yinda et al., 2021; Zheng et al., 2021). All these studies
475 show that intranasal inoculation of K18-hACE2 mice can lead to infection and
476 extensive virus spread in the brain within 6 or 7 days. Infection even stretches into
477 the spinal cord and can basically affect the entire grey matter, including, though only
478 rarely, also the cerebellar cortex (Purkinje cells). This indicates that SARS-CoV-2 has
479 no selective neurotropism.

480 In the present study, intranasala inoculation of mice with a low viral dose (10^3 PFU
481 of the hCoV-2/human/Liverpool/REMRQ0001/2020) resulted in limited CNS infection;
482 it was most pronounced in basal structures of the brain and did not reach the spinal
483 cord. With the higher infectious dose (10^4 PFU) or with IAV pre-infection, we
484 observed widespread extensive viral antigen expression and involvement of the

485 spinal cord. This suggests some dose dependence of virus spread in the CNS, as it
486 was suspected in another study (Yinda et al., 2021), and an effect of prior damage in
487 the respiratory tract (Clark et al., 2021). At the same time, we and others found virus
488 in the olfactory epithelium and in neurons in the olfactory bulb (Carossino et al., 2021;
489 Kumari et al., 2021). Therefore, a rostral to caudal spread of infection with emphasis
490 on basal structures and consequent infection of cortical areas is most likely. This
491 implies a direct neuronal spread of the virus rather than a disseminated pattern which
492 would be consistent with a hematogenous route of infection. A recent ultrastructural
493 examination on SARS-CoV-2 infected human brain organoids is in agreement with
494 these observations, as it provides evidence of virus cell-to-cell-spread beween
495 neurons in the organoids (Song et al., 2021). Many of the SARS-CoV-2 antigen
496 positive neurons of mice of this study are located in areas which are secondary or
497 tertiary connections of the olfactory bulb. This gives further evidence of virus entry via
498 the olfactory bulb, as confirmed in both mice (Carossino et al., 2021; Zheng et al.,
499 2021) and humans (Meinhard et al., 2020) as a natural route of brain infection by
500 SARS-CoV-2. However, many virus-positive regions that are not directly connected
501 to the olfactory system were also identified, providing further evidence of an
502 additional route of viral dissemination (Zheng et al., 2021).
503 Clinical signs consistent with neurological disease have only been reported in one
504 experimental study to date, where mice had shown hunchbacked posture, ruffled fur,
505 tremors and ataxic gait from day 4 pi, and died after day 6. These mice carried very
506 high levels of infectious virus in the brain and showed an encephalitis with
507 perivascular hemorrhage. Neuronal death via apoptosis was suspected (Kumari et
508 al., 2021). Other studies reported perivascular cuffs or vasculitis, neuronal
509 degeneration and necrosis, satellitosis, parenchymal edema, and occasional
510 microthrombi (Oladunni et al., 2020; Carossino et al., 2021; Yinda et al., 2021; Zheng

511 et al., 2021), all at day 7 post infection. The present study confirms that SARS-CoV-2
512 readily infects neurons in the K18-hACE2 mice, with viral protein accumulation in the
513 entire cytoplasm including the cell processes, but does not provide evidence of
514 neuronal cell death in association with infection, indicating that SARS-CoV-2 has no
515 direct cytopathic effect on neurons. This may be due to the lower viral dose, provided
516 that a high viral load would damage neurons directly.

517 Involvement of the spinal cord, which was a prominent feature in our mouse
518 model, has only been reported in a few human cases (Mondal et al., 2020). It might
519 be a so far under-recognized neurological complication, since neuropathological
520 assessments did not go beyond neuroimaging and evaluation of several CSF
521 parameters.

522 Similar to Carossino et al. (2021), the present study did not find evidence of
523 demyelination. Furthermore, axonal damage was not present in the investigated
524 murine brain sections. However, while both axonal damage and demyelination can
525 occur in COVID-19 patients, they are apparently not common neuropathological
526 findings (Kantonen et al., 2020; Reichard et al., 2020; Salomon et al., 2020).

527 Neuronal SARS-CoV-2 infection without obvious neuronal degeneration is
528 reminiscent of other neurotropic and persistent viral infections, like herpes simplex
529 virus (HSV). HSV-1 establishes latency in the mouse model within the earliest stages
530 of acute infection, with the viral genome reaching the neuronal ganglia within the first
531 24 hours of infection (Steiner et al., 1990). Further studies would now be required to
532 determine whether SARS-CoV-2 also establishes latency or whether there is
533 subsequent neuronal damage.

534 Viral infection of neurons is evidently associated with an antiviral response in the
535 mice, as indicated by a reported increase in IFN-α mRNA in the brain from day 5 pi
536 onwards, with a peak of both mRNA and protein on day 6 (Kumari et al., 2021). This

537 is accompanied by an inflammatory response in the brain parenchyma. Similar to a
538 previous study (Oladunni et al., 2020), we observed a mild non-suppurative,
539 macrophage and T cell driven encephalitis (perivascular infiltrates and occasional
540 vasculitis) in all mice that harbored viral antigen in the brains at 7 dpi. This appeared
541 to be slightly more intense with more extensive neuronal virus antigen expression in
542 animals that had received the higher viral dose (10^4 PFU) or had been preinfected
543 with IAV, suggesting some dependence on the infectious dose or easier access to
544 the brain with pre-existing damage due to IAV infection (Clark et al., 2021; Yinda et
545 al., 2021). Transcriptional investigations also confirmed the inflammatory state of the
546 brain, demonstrating an increase in infammatory cytokines and chemokines (IL-6,
547 TNF-α, IFN-γ, IL-1β, MIP-1α.MIP-2, IP-10) in the brain of infected mice (Oladunni et
548 al., 2020; Kumari et al., 2021). This might also explain the activation/hypertrophy of
549 astrocytes in areas with perivascular infiltrates and the diffuse microglial activation
550 and multifocal microgliosis that we and others observed (Winkler et al., 2020;
551 Carossino et al., 2021; Yinda et al., 2021). Both glial cell populations are responsive
552 to proinflammatory signals from endothelial cells, macrophages and/or neurons
553 (Murta et al., 2020). The proinflammatory gene expression program initiated after
554 viral infection would expand neuroinflammation (Murta et al., 2020). Activated
555 microglia may itself undergo a phenotypic shift and display exaggerated release of
556 pro-inflammatory mediators and aberrant phagocytic activity, inducing
557 neurodegeneration (Tremblay et al., 2020). This could explain the diffuse astrogliosis
558 reported from other mouse and human studies (Carossino et al., 2021; Matschke et
559 al., 2020) as well as neuronophagia by microglial cells which was seen in some
560 human COVID-19 patients (Al-Dalahmah et al., 2020) and one mouse study
561 (Carossino et al., 2021).

562 In previous studies we and others have shown that IAV pre-infection of hACE2
563 mice results in more severe SARS-CoV-2 associated pulmonary changes and higher
564 amounts of infectious virus at 6 or 7 days post SARS-CoV-2 infection (Bai et al.,
565 2021; Clark et al., 2021). Interestingly though, viral loads in the brain were not found
566 to be increased (Bai et al., 2021), although we observed higher frequency and more
567 widespread brain infection after the lower SARS-CoV-2 dose in animals that were
568 infected with IAV. Also, the inflammatory response was slightly more intense in these
569 animals. It is currently unclear which direct impact IAV infection has for the
570 subsequent SARS-CoV-2 challenge, but more efficient virus entry could be an option,
571 since IAV infection was shown to upregulate ACE2 expression *in vitro* (Bai et al.,
572 2021).
573 While we did not find evidence of neuronal death, we observed apoptosis of
574 infiltrating lymphocytes, capillary endothelial cells and macrophages/microglial cells
575 in proximity to perivascular infiltrates. As in a previous study (Carossino et al., 2021),
576 none of these cells were found to be SARS-CoV-2 infected. This result is in line with
577 recent findings in SARS-CoV-2 infected human brain organoids which provided
578 evidence that infected neurons do not die but can promote the death of adjacent
579 uninfected cells (Song et al., 2021). Using single cell RNA sequencing, the study
580 showed that SARS-CoV-2 infected cells in the organoids were in a hypermetabolic
581 state, whereas uninfected cells nearby were in a catabolic state and a hypoxic
582 environment, as shown by HIF1α expression (Song et al., 2021). The same may be
583 true for the brain of K18-hACE2 mice with widespread neuronal SARS-CoV-2
584 infection. Also, coupled proliferation and apoptosis are assumed to maintain the quite
585 rapid turnover of microglia in the adult brain (Askew et al., 2017). We did not
586 determine the proliferation rate in this study, but such “physiological” turnover should
587 be considered when interpreting microglial apoptosis in SARS-CoV-2 infected mice.

588 Several morphological changes in the mice used in the present study recapitulate
589 findings reported in brains of human COVID-19 patients, like mild perivascular
590 inflammatory infiltrates (Solomon et al., 2020) and microgliosis (Schuhrink et al.,
591 2020). In the mice, the inflammatory processes were only mild and more pronounced
592 in frontal regions like caudoputamen and the thalamus/hypothalamus region as well
593 as the hippocampal area. Further vascular lesions apart from vasculitis/endotheliitis,
594 like ischemic infarcts (Kantonen et al., 2020; Song et al., 2021) or microthrombi
595 (Fabbri et al., 2020) that seem to be frequent in fatal human COVID-19 cases, are
596 obviously not a regular feature in this mouse model, since only two studies reported
597 occasional microthrombi in the brain (Yinda et al., 2021; Zheng et al., 2021). This
598 could be due to the lack of endothelial cell infection in the brain of the mice, whereas
599 it was seen in association with fresh ischemic infarcts in the brain of a COVID-19
600 patient (Meinhardt et al., 2021; Song et al., 2021). Interestingly, the presence of virus
601 in the brain of the human patients is apparently not consistently associated with
602 leukocyte infiltration, indicating that SARS-CoV-2 does not necessarily induce an
603 immune response like other neurotropic viruses (Song et al., 2021).
604 The main host receptor for SARS-CoV-2 is the human angiotensin-converting
605 enzyme 2 (hACE2). While a study in the brain of fatal human COVID-19 cases
606 showed ACE2 expression in cortical neurons and found evidence that ACE2 is
607 required for infection of human brain organoids (Song et al., 2021), neuroinvasion
608 and spread in the K18-hACE2 mice is apparently not directly dependent upon ACE2
609 expression, because the virus does not infect all ACE2 expressing cells and does
610 infect cells without apparent ACE2 expression (Carossino et al., 2021). Indeed, in line
611 with the findings of previous studies we only detected ACE2 protein expression in
612 capillary endothelial cells, ependymal cells and choroid plexus epithelium in the brain
613 and spinal cord, in the absence of detectable viral antigen (Carossini et al., 2021;

614 Clark et al., 2021; Song et al., 2021). In human COVID-19 patients, the endothelium
615 of capillaries in kidney, liver, heart, lung and small intestine was shown to become
616 infected, and this was associated with an endotheliitis (Varga et al., 2020).
617 Furthermore, ultrastructural examination of the brain of one human patient found viral
618 particles in small vesicles of endothelial cells, suspecting an additional
619 hematogenous route of brain infection (Paniz-Mondolfi et al., 2020). Indeed, using
620 intravenously injected radioiodinated SARS-CoV-2 S1 it has been shown that the
621 viral protein can cross the BBB, and likely by absorptive transcytosis (Rhea et al.,
622 2020). It may hence be due to the fact that endothelial ACE2 expression in the K18-
623 hACE2 mice represents only the murine protein (Carassino et al., 2021) that the brain
624 endothelium of the mice does not become infected by SARS-CoV-2.
625 Based on current knowledge, it seems likely that in COVID-19 patients the virus can
626 access the brain in several ways. In severe COVID-19, viremia could allow access to
627 the brain via the vasculature (Colagrossi et al., 2021). With the platelet hyperactivity
628 in critically ill patients (Comer et al., 2021) and abnormal blood clotting or unusual
629 thrombotic presentations (Helms et al., 2020b, Klok et al., 2020) this might lead to the
630 ischemic changes described in a proportion of fatal cases, without viral infection of
631 neurons. This might not be mirrored by the murine model as viremia may not occur
632 (Yinda et al., 2021). In mild COVID-19, i.e. without viremia, infection of the brain via
633 the olfactory bulb and possible other neurogenic routes could occur. This would then
634 lead to exclusive neuronal infection and an only mild inflammatory response. It might
635 be this scenario that explains the loss of taste and smell and severe headaches
636 reported in patients with mild disease.
637 The murine model does not fulfil all morphological criteria of acute human
638 neurological COVID-19. However, brain infection following a lower dose of intranasal
639 challenge might represent a mouse model for chronic/long COVID-19 studies. The

640 pathogenesis of this sequel of the acute disease is still unknown, but fatigue, muscle
641 aches, breathlessness, and headaches are the most frequently reported symptoms
642 (Dennis et al., 2020; Brodin, 2021). A persistent low-grade smoldering inflammatory
643 response to newly budding virions might be central to the condition. Also,
644 degeneration or impaired function of neuronal and glial cells that are cardinal for the
645 physiological function of the brain might be an option (Baig, 2020). A mild inadequate
646 immune response with persistent viral load and viral evasion of the immune
647 surveillance are suspected key factors (Baig, 2020). This is supported by the fact that
648 COVID-19 patients still exhibit a significant remaining inflammatory response in the
649 serum at 40-60 days post infection (Doykov et al., 2020). Further investigations of the
650 inflammatory response at transcriptome and translational level in the murine model
651 could provide further insights.
652 These data also have important implications for the development of therapeutic
653 interventions. Firstly, the endothelium and astrocyte foot processes represent key
654 components of the BBB, protecting the brain from accumulation of endo- and xeno-
655 biotics. Future studies should address the consequences of infection for maintenance
656 of barrier integrity to mitigate potential inadvertant delivery of neurotoxic agents that
657 wouldn't otherwise permeate the brain. Secondly, several studies have already
658 sought to understand pulmonary distribution of postulated therapeutic interventions
659 (Arshad et al., 2020; Hanafin et al., 2021; Rajoli et al., 2021) but robust efficacy of
660 antivirals and/or immunomodulatory agents may also necessitate adequate exposure
661 within the CNS. Notably, the repurposed antivirals remdesivir, favipiravir and
662 molnupiravir exhibit low concentrations in the brain relative to plasma in preclinical
663 species (Bocan et al., 2019; Painter et al., 2019; EMA, 2020; Jorgensen et al., 2020).
664 Furthermore, dexamethasone also exhibits low brain penetration in mice with an
665 intact BBB, but this increases in mice genetically engineered to be absent a critical

666 drug transporter, P-glycoprotein (Meijer et al., 1998). Further work is required to
667 define the importance of brain penetration of therapeutics being investigated as
668 interventions across the spectrum of disease from prevention, mild, moderate, severe
669 to long COVID-19.
670

671 **Conclusions**

672 Despite widespread neuronal infection, pathomorphological changes of the course of
673 disease consisted of mild lymphohistiocytic inflammation and microglial activation.
674 Solely neuronal cells were infected which supported the infectious route via the
675 olfactory epithelium, olfacory bulb and transsynaptic spreading. The limited
676 expression of ACE2 raises the question for ACE2-independent pathogenetic
677 mechanisms to explain the neurotropism of the virus. Microgliosis and immune cell
678 apoptosis were main pathological features in our study indicating a potential
679 important role of microglial cells in the pathogenesis of neuromanifestation in COVID-
680 19.
681

682 **Acknowledgements**
683 We are grateful to the technical staff in the Histology Laboratory, Institute of
684 Veterinary Pathology, Vetsuisse Faculty, University of Zurich (IVPZ), for excellent
685 technical support. This work was funded in part by the US Food and Drug
686 Administration (USA) 75F40120C00085, Characterization of severe coronavirus
687 infection in humans and model systems for medical countermeasure development
688 and evaluation (JAH). Work in the lab is also supported by MRC grant
689 MR/W005611/1, G2P-UK; A National Virology Consortium to address phenotypic
690 consequences of SARSCoV-2 genomic variation (JPS and JAH).
691
692

693 **CONFLICT OF INTEREST**
694 The authors declare that they have no conflict of interest.
695

REFERENCES

Alam SB, Willows S, Kulka M, Sandhu JK, 2020. Severe acute respiratory syndrome coronavirus 2 may be an underappreciated pathogen of the central nervous system. Eur J Neurol 27(11):2348-2360. doi: 10.1111/ene.14442.

Al-Dalahmah O, Thakur KT, Nordvig AS, Prust ML, Roth W, Lignelli A, Uhlemann AC, Miller EH, Kunnath-Velayudhan S, Del Portillo A, Liu Y, Hargus G, Teich AF, Hickman RA, Tanji K, Goldman JE, Faust PL, Canoll P, 2020. Neuronophagia and microglial nodules in a SARS-CoV-2 patient with cerebellar hemorrhage. Acta Neuropathol Commun 8(1):147. doi: 10.1186/s40478-020-01024-2.

Al-Sarraj S, Troakes C, Hanley B, Osborn M, Richardson MP, Hotopf M, Bullmore E, Everall IP, 2021. Invited Review: The spectrum of neuropathology in COVID-19. Neuropathol Appl Neurobiol 47(1):3-16. doi: 10.1111/nan.12667.

Arshad U, Pertinez H, Box H, Tatham L, Rajoli RKR, Curley P, Neary M, Sharp J, Liptrott NJ, Valentijn A, David C, Rannard SP, O'Neill PM, Aljayyoussi G, Pennington SH, Ward SA, Hill A, Back DJ, Khoo SH, Bray PG, Biagini GA, Owen A, 2021. Prioritization of anti-SARS-Cov-2 drug repurposing opportunities based on plasma and target site concentrations derived from their established human pharmacokinetics. Clin Pharmacol Ther 108(4):775-790. doi: 10.1002/cpt.1909.

Askew K, Li K, Olmos-Alonso A, Garcia-Moreno F, Liang Y, Richardson P, Tipton T, Chapman MA, Riecken K, Beccari S, Sierra A, Molnár Z, Cragg MS, Garaschuk O, Perry VH, Gomez-Nicola D, 2017. Coupled proliferation and apoptosis maintain the rapid turnover of microglia in the adult brain. Cell Rep. 18(2):391-405. doi: 10.1016/j.celrep.2016.12.041.

Bai L, Zhao Y, Dong J, Liang S, Guo M, Liu X, Wang X, Huang Z, Sun X, Zhang Z, Dong L, Liu Q, Zheng Y, Niu D, Xiang M, Song K, Ye J, Zheng W, Tang Z, Tang M, Zhou Y, Shen C, Dai M, Zhou L, Chen Y, Yan H, Lan, K Xu, K, 2021. Coinfection with influenza A virus enhances SARS-CoV-2 infectivity. Cell Res 1-9. doi: 10.1038/s41422-021-00473-1.

Baig AM, 2020. Deleterious outcomes in long-hauler COVID-19: The effects of SARS-CoV-2 on the CNS in chronic COVID syndrome. ACS Chem Neurosci 11(24):4017-4020. doi: 10.1021/acschemneuro.0c00725.

Bocan TM, Basuli F, Stafford RG, Brown JL, Zhang X, Duplantier AJ, Swenson RE, 2019. Synthesis of [^{18}F]Favipiravir and biodistribution in C3H/HeN Mice as assessed by positron emission tomography. Sci Rep 9(1):1785. doi: 10.1038/s41598-018-37866-z.

Brodin P, 2021. Immune determinants of COVID-19 disease presentation and severity. Nat Med 27, 28-33. doi: 10.1038/s41591-020-01202-8.

Bussani R, Schneider E, Zentilin L, Collesi C, Ali H, Braga L, Volpe MC, Colliva A, Zanconati F, Berlot G, Silvestri F, Zacchigna S, Giacca M, 2020. Persistence of viral RNA, pneumocyte syncytia and thrombosis are hallmarks of advanced COVID-19 pathology. EBioMedicine 61:103104. doi: 10.1016/j.ebiom.2020.103104.

Cantuti-Castelvetri L, Ojha R, Pedro LD, Djannatian M, Franz J, Kuivanen S, van der Meer F, Kallio K, Kaya T, Anastasina M, Smura T, Levanov L, Szirovicza L, Tobi A, Kallio-Kokko H, Österlund P, Joensuu M, Meunier FA, Butcher SJ, Winkler MS, Mollenhauer B, Helenius A, Gokce O, Teesalu T, Hepojoki J, Vapalahti O, Stadelmann C, Balistreri G, Simons M, 2020. Neuropilin-1 facilitates SARS-CoV-2 cell entry and infectivity. Science 370(6518):856-860. doi: 10.1126/science.abd2985.

Carossino M, Montanaro P, O'Connell A, Kenney D, Gertje H, Grosz KA, Kurnick SA, Bosmann M, Saeed M, Balasuriya UBR, Douam F, Crossland NA, 2021. Fatal neuroinvasion of SARS-CoV-2 in K18-hACE2 mice is partially dependent on hACE2 expression. bioRxiv preprint doi: doi.org/10.1101/2021.01.13.425144. version posted January 15, 2021.

Clark JJ, Penrice-Randal R, Sharma P, Kipar A, Dong X, Davidson A, Kavanagh Williamson M, Matthews DA, Turtle L, Prince T, Hughes GL, Patterson EI, Shawli G, Subramaniam K, Sharp J, McLaughlin L, Zhou E-M, Turner JD, Marriott AE, Colombo S, Pennington SH, Biagini G, Owen A, Hiscox JA, Stewart JP, 2021. Sequential infection with influenza A virus followed by severe acute respiratory syndrome coronavirus 2 (SARS-CoV-2) leads to more severe disease and encephalitis in a mouse model of COVID-19. bioRxiv preprint doi: 10.1101/2020.10.13.334532.

Colagrossi L, Antonello M, Renica S, Merli M, Matarazzo E, Travi G, Vecchi M, Colombo J, Muscatello A, Grasselli G, Molteni SN, Scaravilli V, Cattaneo E, Fanti D, Vismara C, Bandera A, Gori A, Puoti M, Cento V, Alteri C, Perno CF, 2021. SARS-CoV-2 RNA in plasma samples of COVID-19 affected individuals: a cross-sectional proof-of-concept study. BMC Infect Dis 21(1):184. doi: 10.1186/s12879-021-05886-2.

Comer SP, Cullivan S, Szklanna PB, Weiss L, Cullen S, Kelliher S, Smolenski A, Murphy C, Altaie H, Curran J, O'Reilly K, Cotter AG, Marsh B, Gaine S, Mallon P, McCullagh B, Moran N, Ní Áinle F, Kevane B, Maguire PB, COCOON study investigators, 2021. COVID-19 induces a hyperactive phenotype in circulating platelets. PLoS Biol 19(2):e3001109. doi: 10.1371/journal.pbio.3001109.

Deigendesch N, Sironi L, Kutza M, Wischnewski S, Fuchs V, Hench J, Frank A, Nienhold R, Mertz KD, Cathomas G, Matter MS, Siegemund M, Tolnay M, Schirmer L, Pröbstel AK, Tzankov A, Frank S. Correlates of critical illness-related encephalopathy predominate postmortem COVID-19 neuropathology, 2020. Acta Neuropathol 140(4):583-586. doi: 10.1007/s00401-020-02213-y.

Dennis A, Wamil M, Kapur S, Alberts J, Badley AD, Decker GA, Rizza SA, Banerjee R, Banerjee A, 2020. Multi-organ impairment in low-risk individuals with long COVID. medRxiv 2020.10.14.20212555. doi: 10.1101/2020.10.14.20212555

Doykov I, Hällqvist J, Gilmour KC, Grandjean L, Mills K, Heywood WE, 2020. 'The long tail of Covid-19' - The detection of a prolonged inflammatory response after a SARS-CoV-2 infection in asymptomatic and mildly affected patients. F1000Res 9:1349. doi: 10.12688/f1000research.27287.2. PMID: 33391730; PMCID: PMC7745182.

EMA (European Medicines Agency), 2020. Remdesivir Gilead – Summary on compassionate use. EMA/178637/2020

Fabbri VP, Foschini MP, Lazzarotto T, Gabrielli L, Cenacchi G, Gallo C, Aspide R, Frascaroli G, Cortelli P, Riefolo M, Giannini C, D'Errico A, 2021. Brain ischemic injury in COVID-19-infected patients: a series of 10 post-mortem cases. Brain Pathol 31(1):205-210. doi: 10.1111/bpa.12901.

Golden JW, Cline CR, Zeng X, Garrison AR, Carey BD, Mucker EM,White LE, Shamblin JD, Brocato RL, Liu J, Babka AM, Rauch HB, Smith JM, Hollidge BS, Fitzpatrick C, Badger CV, Hooper JW, 2020. Human angiotensin-converting enzyme 2 transgenic mice infected with SARS-CoV-2 develop severe and fatal respiratory disease. JCI Insight 5(19):e142032. doi: 10.1172/jci.insight.142032.

Helms J, Kremer S, Merdji H, Clere-Jehl R, Schenck M, Kummerlen C, Collange O, Boulay C, Fafi-Kremer S, Ohana M, Anheim M, Meziani F, 2020a. Neurologic features in severe SARS-CoV-2 infection. N Engl J Med 382(23):2268-2270. doi: 10.1056/NEJMc2008597.

Helms J, Tacquard C, Severac F, Leonard-Lorant I, Ohana M, Delabranche X, Merdji H, Clere-Jehl R, Schenck M, Fagot Gandet F, Fafi-Kremer S, Castelain V, Schneider F, Grunebaum L, Anglés-Cano E, Sattler L, Mertes PM, Meziani F; CRICS TRIGGERSEP Group, 2020b. High risk of thrombosis in patients with severe SARS-CoV-2 infection: a multicenter prospective cohort study. Intensive Care Med 46(6):1089-1098. doi: 10.1007/s00134-020-06062-x.

Hoffmann M, Kleine-Weber H, Schroeder S, Kruger N, Herrler T, Erichsen S, Schiergens TS, Herrler G, Wu NH, Nitsche A, Muller MA, Drosten C, Pohlmann S, 2020. SARS-CoV-2 cell entry depends on ACE2 and TMPRSS2 and is blocked by a clinically proven protease inhibitor. Cell 181:271-280 e278. doi: 10.1016/j.cell.2020.02.052

Huang YH, Jiang D, Huang JT, 2020. SARS-CoV-2 detected in cerebrospinal fluid by PCR in a case of COVID-19 encephalitis. Brain Behav Immun 87:149. doi: 10.1016/j.bbi.2020.05.012.

Jaunmuktane Z, Mahadeva U, Green A, Sekhawat V, Barrett NA, Childs L, Shankar-Hari M, Thom M, Jäger HR, Brandner S, 2020. Microvascular injury and hypoxic damage: emerging neuropathological signatures in COVID-19. Acta Neuropathol 140(3):397-400. doi: 10.1007/s00401-020-02190-2.

Jorgensen SCJ, Kebriaei R, Dresser LD. Remdesivir: Review of pharmacology, pre-clinical data, and emerging clinical experience for COVID-19, 2020. Pharmacotherapy 40(7):659-671. doi: 10.1002/phar.2429.

Kantonen J, Mahzabin S, Mäyränpää MI, Tynninen O, Paetau A, Andersson N, Sajantila A, Vapalahti O, Carpén O, Kekäläinen E, Kantele A, Myllykangas L. Neuropathologic features of four autopsied COVID-19 patients, 2020. Brain Pathol 30(6):1012-1016. doi: 10.1111/bpa.12889.

Klok FA, Kruip MJHA, van der Meer NJM, Arbous MS, Gommers D, Kant KM, Kaptein FHJ, van Paassen J, Stals MAM, Huisman MV, Endeman H, 2020. Confirmation of the high cumulative incidence of thrombotic complications in critically ill ICU patients with

848 COVID-19: An updated analysis. Thromb Res 191:148-150. doi:
849 10.1016/j.thromres.2020.04.041.
850
851 Kumari P, Rothan HA, Natekar JP, Stone S, Pathak H, Strate PG, Arora K, Brinton MA,
852 Kumar M, 2021. Neuroinvasion and encephalitis following intranasal inoculation of
853 SARS-CoV-2 in K18-hACE2 mice. Viruses 13:132. doi: 10.3390/v13010132.
854
855 Lavi E, Cong L, 2020. Type I astrocytes and microglia induce a cytokine response in
856 an encephalitic murine coronavirus infection. Exp Mol Pathol 115:104474. doi:
857 10.1016/j.yexmp.2020.104474.
858
859 Mahalaxmi I, Kaavya J, Mohana Devi S, Balachandar V, 2021. COVID-19 and olfactory
860 dysfunction: A possible associative approach towards neurodegenerative diseases. J
861 Cell Physiol 236(2):763-770. doi: 10.1002/jcp.29937.
862
863 Mao L, Jin H, Wang M, Hu Y, Chen S, He Q, Chang J, Hong C, Zhou Y, Wang D, Miao
864 X, Li Y, Hu B, 2020. Neurologic Manifestations of Hospitalized Patients With
865 Coronavirus Disease 2019 in Wuhan, China. JAMA Neurol 77(6):683-690. doi:
866 10.1001/jamaneurol.2020.1127.
867
868 Matschke J, Lütgehetmann M, Hagel C, Sperhake JP, Schröder AS, Edler C,
869 Mushumba H, Fitzek A, Allweiss L, Dandri M, Dottermusch M, Heinemann A, Pfefferle
870 S, Schwabenland M, Sumner Magruder D, Bonn S, Prinz M, Gerloff C, Püschel K,
871 Krasemann S, Aepfelbacher M, Glatzel M. Neuropathology of patients with COVID-19
872 in Germany: a post-mortem case series, 2020. Lancet Neurol 19(11):919-929. doi:
873 10.1016/S1474-4422(20)30308-2.
874
875 McCray PB Jr, Pewe L, Wohlford-Lenane C, Hickey M, Manzel L, Shi L, Netland J, Jia
876 HP, Halabi C, Sigmund CD, Meyerholz DK, Kirby P, Look DC, Perlman S, 2007. Lethal
877 infection of K18-hACE2 mice infected with severe acute respiratory syndrome
878 coronavirus. J Virol 81:813-821. doi:10.1128/JVI.02012-06.
879
880 Meijer OC, de Lange ECM, Breimer DD, de Boer AG, Workel JO, de Kloet ER, 1998.
881 Penetration of dexamethasone into brain glucocorticoid targets is enhanced in mdr1A
882 P-glycoprotein knockout mice. Endocrinology 139(4):1789-1793. doi:
883 10.1210/endo.139.4.5917.
884
885 Meinhardt J, Radke J, Dittmayer C, Franz J, Thomas C, Mothes R, Laue M, Schneider
886 J, Brünink S, Greuel S, Lehmann M, Hassan O, Aschman T, Schumann E, Chua RL,
887 Conrad C, Eils R, Stenzel W, Windgassen M, Rößler L, Goebel HH, Gelderblom HR,
888 Martin H, Nitsche A, Schulz-Schaeffer WJ, Hakroush S, Winkler MS, Tampe B,
889 Scheibe F, Körtvélyessy P, Reinhold D, Siegmund B, Kühl AA, Elezkurtaj S, Horst D,
890 Oesterhelweg L, Tsokos M, Ingold-Heppner B, Stadelmann C, Drosten C, Corman VM,
891 Radbruch H, Heppner FL, 2021. Olfactory transmucosal SARS-CoV-2 invasion as a
892 port of central nervous system entry in individuals with COVID-19. Nat Neurosci 24:
893 168-175 doi: 10.1038/s41593-020-00758-5.
894
895 Michael BD, Bricio-Moreno L, Sorensen EW, Miyabe Y, Lian J, Solomon T, Kurt-Jones
896 EA, Luster AD, 2020. Astrocyte- and neuron-derived CXCL1 drives neutrophil
897 transmigration and blood-brain barrier permeability in viral encephalitis. Cell Rep. 2020
898 September 15; 32(11): 108150. doi:10.1016/j.celrep.2020.108150

Mondal R, Deb S, Shome G, Ganguly U, Lahiri D, Leon JB, 2020. Spectrum of spinal cord involvement in COVID-19: A systematic review. medRxiv 2020.09.29.20203554. doi: 10.1101/2020.09.29.20203554.

Moriguchi T, Harii N, Goto J, Harada D, Sugawara H, Takamino J, Ueno M, Sakata H, Kondo K, Myose N, Nakao A, Takeda M, Haro H, Inoue O, Suzuki-Inoue K, Kubokawa K, Ogihara S, Sasaki T, Kinouchi H, Kojin H, Ito M, Onishi H, Shimizu T, Sasaki Y, Enomoto N, Ishihara H, Furuya S, Yamamoto T, Shimada S, 2020. A first case of meningitis/encephalitis associated with SARS-Coronavirus-2. Int J Infect Dis 94:55-58. doi: 10.1016/j.ijid.2020.03.062.

Murta V, Farías MI, Pitossi FJ, Ferrari CC, 2015. Chronic systemic IL-1β exacerbates central neuroinflammation independently of the blood-brain barrier integrity. J Neuroimmunol 278:30-43. doi: 10.1016/j.jneuroim.2014.11.023.

Murta V, Ferrari C, 2016. Peripheral inflammation and demyelinating diseases. Adv Exp Med Biol 949:263-285. doi: 10.1007/978-3-319-40764-7_13.

Murta V, Villarreal A, Ramos AJ, 2020. Severe Acute Respiratory Syndrome Coronavirus 2 impact on the central nervous system: Are astrocytes and microglia main players or merely bystanders? ASN Neuro 12:1759091420954960. doi: 10.1177/1759091420954960.

Najjar, S Najjar A, Chong DJ, Pramanik BK, Kirsch C, Kuzniecky RI, Pacia SV, Azhar S, 2020. Central nervous system complications associated with SARS-CoV-2 infection: integrative concepts of pathophysiology and case reports. J Neuroinflammation 17: 231. doi: 10.1186/s12974-020-01896-0.

Oladunni FS, Park J-G, Pino PA, Gonzalez O, Akhter A, Allué-Guardia A, Olmo-Fontánez A, Gautam S, Garcia-Vilanova A, Ye C, Chiem K, Headley C, Dwivedi V, Parodi LM, Alfson KJ, Staples HM, Schami A, Garcia JI, Whigham A, Platt RN, Gazi M, Martinez J, Chuba C, Earley S, Rodriguez OH, Davis Mdaki S, Kavelish KN, Escalona R, Hallam CRA, Christie C, Patterson JL, Anderson TJC, Carrion R, Dick EJ, Hall-Ursone S, Schlesinger LS, Alvarez X, Kaushal D, Giavedoni LD, Turner J, Martinez-Sobrido L, Torrelles JB, 2020. Lethality of SARS-CoV-2 infection in K18 human angiotensin-converting enzyme 2 transgenic mice. Nat Commun 11(1):6122. doi: 10.1038/s41467-020-19891-7.

Oxley TJ, Mocco J, Majidi S, Kellner CP, Shoirah H, Singh IP, De Leacy RA, Shigematsu T, Ladner TR, Yaeger KA, Skliut M, Weinberger J, Dangayach NS, Bederson JB, Tuhrim S, Fifi JT, 2020. Large-vessel stroke as a presenting feature of COVID-19 in the young. N Engl J Med 382(20):e60. doi: 10.1056/NEJMc2009787.

George R. Painter, Richard A. Bowen, Gregory R. Bluemling, John DeBergh, Vindhya Edpuganti, Prabhakar R. Gruddanti, David B. Guthrie, Michael Hager, Damien L. Kuiper, Mark A. Lockwood, Deborah G. Mitchell, Michael G. Natchus, Zachary M. Sticher, Alexander A. Kolykhalov. The prophylactic and therapeutic activity of a broadly active ribonucleoside analog in a murine model of intranasal venezuelan equine encephalitis virus infection. Antiviral Research, Volume 171, 2019, 104597, doi: 10.1016/j.antiviral.2019.104597.

Paniz-Mondolfi A, Bryce C, Grimes Z, Gordon RE, Reidy J, Lednicky J, Sordillo EM, Fowkes M, 2020. Central nervous system involvement by severe acute respiratory syndrome coronavirus-2 (SARS-CoV-2). J Med Virol 92(7):699-702. doi: 10.1002/jmv.25915.

Patterson EI, Prince T, Anderson ER, Casas-Sanchez A, Smith SL, Cansado-Utrilla C, Solomon T, Griffiths MJ, Acosta-Serrano Á, Turtle L, Hughes G, 2020. Methods of inactivation of SARS-CoV-2 for downstream biological assays. J Infect Dis 222(9):1462-1467. doi:10.1093/infdis/jiaa507.

Perry VH, Cunningham C, Holmes C, 2007. Systemic infections and inflammation affect chronic neurodegeneration. Nat Rev Immunol 7(2):161-7. doi: 10.1038/nri2015.

Perry VH, Teeling J, 2013. Microglia and macrophages of the central nervous system: the contribution of microglia priming and systemic inflammation to chronic neurodegeneration. Semin Immunopathol 35(5):601-12. doi: 10.1007/s00281-013-0382-8.

Poyiadji N, Shahin G, Noujaim D, Stone M, Patel S, Griffith B, 2020. COVID-19-associated acute hemorrhagic necrotizing encephalopathy: Imaging features. Radiology 296(2):E119-E120. doi: 10.1148/radiol.2020201187.

Puelles VG, Lütgehetmann M, Lindenmeyer MT, Sperhake JP, Wong MN, Allweiss L, Chilla S, Heinemann A, Wanner N, Liu S, Braun F, Lu S, Pfefferle S, Schröder AS, Edler C, Gross O, Glatzel M, Wichmann D, Wiech T, Kluge S, Pueschel K, Aepfelbacher M, Huber TB, 2020. Multiorgan and renal tropism of SARS-CoV-2. N Engl J Med 383(6):590-592. doi: 10.1056/NEJMc2011400.

Rajoli RKR, Pertinez H, Arshad U, Box H, Tatham L, Curley P, Neary M, Sharp J, Liptrott NJ, Valentijn A, David C, Rannard SP, Aljayyoussi G, Pennington SH, Hill A, Boffito M, Ward SA, Khoo SH, Bray PG, O'Neill PM, Hong WD, Biagini GA, Owen A. Dose prediction for repurposing nitazoxanide in SARS-CoV-2 treatment or chemoprophylaxis, 2021. Br J Clin Pharmacol. 2021 Apr;87(4):2078-2088. doi: 10.1111/bcp.14619. Epub 2020 Dec 1. PMID: 33085781.

Reichard RR, Kashani KB, Boire NA, Constantopoulos E, Guo Y, Lucchinetti CF, 2020. Neuropathology of COVID-19: a spectrum of vascular and acute disseminated encephalomyelitis (ADEM)-like pathology. Acta Neuropathol 140:1-6. doi: 10.1007/s00401-020-02166-2.

Rhea EM, Logsdon AF, Hansen KM, Williams LM, Reed MJ, Baumann KK, Holden SJ, Raber J, Banks WA, Erickson MA, 2020. The S1 protein of SARS-CoV-2 crosses the blood-brain barrier in mice. Nat Neurosci 24:368-378. doi: 10.1038/s41590-020-0778-2.

Salguero FJ, White AD, Slack GS, Fotheringham SA, Bewley KR, Gooch KE, Longet S, Humphries HE, Watson RJ, Hunter L, Ryan KA, Hall Y, Sibley L, Sarfas C, Allen L, Aram M, Brunt E, Brown P, Buttigieg KR, Cavell BE, Cobb R, Coombes NS, Darby A, Daykin-Pont O, Elmore MJ, Garcia-Dorival I, Gkolfinos K, Godwin KJ, Gouriet J, Halkerston R, Harris DJ, Hender T, Ho CMK, Kennard CL, Knott D, Leung S, Lucas V,

Mabbutt A, Morrison AL, Nelson C, Ngabo D, Paterson J, Penn EJ, Pullan S, Taylor I, Tipton T, Thomas S, Tree JA, Turner C, Vamos E, Wand N, Wiblin NR, Charlton S, Dong X, Hallis B, Pearson G, Rayner EL, Nicholson AG, Funnell SG, Hiscox JA, Dennis MJ, Gleeson FV, Sharpe S, Carroll MW, 2021. Comparison of rhesus and cynomolgus macaques as an infection model for COVID-19. Nat Commun 12(1):1260. doi: 10.1038/s41467-021-21389-9.

Saura-Martinez H, Al-Saadi M, Stewart JP, Kipar K, 2021. Sheep-associated malignant catarrhal fever: role of latent virus and macrophages in vasculitis. Vet Pathol 58(2): 332-345. doi: 10.1177/0300985820978310.

Schurink B, Roos E, Radonic T, Barbe E, Bouman CSC, de Boer HH, de Bree GJ, Bulle EB, Aronica EM, Florquin S, Fronczek J, Heunks LMA, de Jong MD, Guo L, du Long R, Lutter R, Molenaar PCG, Neefjes-Borst EA, Niessen HWM, van Noesel CJM, Roelofs JJTH, Snijder EJ, Soer EC, Verheij J, Vlaar APJ, Vos W, van der Wel NN, van der Wal AC, van der Valk P, Bugiani M, 2020. Viral presence and immunopathology in patients with lethal COVID-19: a prospective autopsy cohort study. Lancet Microbe 1(7):e290-e299. doi: 10.1016/S2666-5247(20)30144-0.

Solomon IH, Normandin E, Bhattacharyya S, Mukerji SS, Keller K, Ali AS, Adams G, Hornick JL, Padera RF Jr, Sabeti P, 2020. Neuropathological features of Covid-19. N Engl J Med 383(10):989-992. doi: 10.1056/NEJMc2019373.

Song E, Zhang C, Israelow B, Lu-Culligan A, Prado AV, Skriabine S, Lu P, Weizman OE, Liu F, Dai Y, Szigeti-Buck K, Yasumoto Y, Wang G, Castaldi C, Heltke J, Ng E, Wheeler J, Alfajaro MM, Levavasseur E, Fontes B, Ravindra NG, Van Dijk D, Mane S, Gunel M, Ring A, Kazmi SAJ, Zhang K, Wilen CB, Horvath TL, Plu I, Haik S, Thomas JL, Louvi A, Farhadian SF, Huttner A, Seilhean D, Renier N, Bilguvar K, Iwasaki A, 2021. Neuroinvasion of SARS-CoV-2 in human and mouse brain. J Exp Med 218(3):e20202135. doi: 10.1101/2020.06.25.169946

Steiner I, Spivack JG, Deshmane SL, Ace CI, Preston CM, Fraser NW, 1990. A herpes simplex virus type 1 mutant containing a nontransinducing Vmw65 protein establishes latent infection in vivo in the absence of viral replication and reactivates efficiently from explanted trigeminal ganglia. J Virol 64:1630-1638. doi: 10.1128/JVI.64.4.1630-1638.1990.

Swanson PA 2nd, McGavern DB, 2015. Viral diseases of the central nervous system. Curr Opin Virol 11:44-54. doi: 10.1016/j.coviro.2014.12.009.

Tremblay ME, Madore C, Bordeleau M, Tian L, Verkhratsky A, 2020. Neuropathobiology of COVID-19: The role for glia. Front Cell Neurosci 14:592214. doi: 10.3389/fncel.2020.592214.

Varga Z, Flammer AJ, Steiger P, Haberecker M, Andermatt R, Zinkernagel AS, Mehra MR, Schuepbach RA, Ruschitzka F, Moch H, 2020. Endothelial cell infection and endotheliitis in COVID-19. The Lancet 395(10234):1417-1418. doi: 10.1016/ S0140-6736(20)30937-5.

Vargas G, Medeiros Geraldo LH, Gedeão Salomão N, Viana Paes M, Regina Souza Lima F, Carvalho Alcantara Gomes F, 2020. Severe acute respiratory syndrome

coronavirus 2 (SARS-CoV-2) and glial cells: Insights and perspectives. Brain Behav Immun Health 7:100127. doi: 10.1016/j.bbih.2020.100127.

von Weyhern CH, Kaufmann I, Neff F, Kremer M, 2020. Early evidence of pronounced brain involvement in fatal COVID-19 outcomes. Lancet 395(10241):e109. doi: 10.1016/S0140-6736(20)31282-4.

Wang Q, Ding SL, Li Y, Royall J, Feng D, Lesnar P, Graddis N, Naeemi M, Facer B, Ho A, Dolbeare T, Blanchard B, Dee N, Wakeman W, Hirokawa KE, Szafer A, Sunkin SM, Oh SW, Bernard A, Phillips JW, Hawrylycz M, Koch C, Zeng H, Harris JA, Ng L, 2020. The Allen Mouse Brain Common Coordinate Framework: A 3D reference atlas. Cell 181(4):936-953.e20. doi: 10.1016/j.cell.2020.04.007.

Winkler ES, Bailey AL, Kafai NM, Nair S, McCune BT, Yu J, Fox JM, Chen RE, Earnest JT, Keeler SP, Riter JH, Kang L-I, Dort S, Robichaud A, Head R, Holtzmann MJ, Diamond MS, 2020. SARS-CoV-2 infection of human ACE2-transgenic mice causes severe lung inflammation and impaired function. Nature Immunol 21:1327-1335. doi: 10.1038/s41590-020-0778-2.

Yinda CK, Port JR, Bushmaker T, Offei Owusu I, Purushotham JN, Avanzato VA, Fischer RJ, Schulz JE, Holbrook MG, Hebner MJ, Rosenke R, Thomas T, Marzi A, Best SM, de Wit E, Shaia C, can Doremalen N, Munster VJ, 2021. K18-hACE2 mice develop respiratory disease resembling severe COVID-19. PLoS Pathog 17(1): e1009195. doi: 10.1371/journal.ppat.1009195.

Zhang S, Liu Y, Wang X, Yang L, Li H, Wang Y, Liu M, Zhao X, Xie Y, Yang Y, Zhang S, Fan Z, Dong J, Yuan Z, Ding Z, Zhang Y, Hu L, 2020. SARS-CoV-2 binds platelet ACE2 to enhance thrombosis in COVID-19. J Hematol Oncol 13(1):120. doi: 10.1186/s13045-020-00954-7.

Zheng J, Wong LYR, Li K, Verma AK, Ortiz ME, Wohlford-Lenane C, Leidinger MR, Knudson CM, Meyerholz DK, McCray Jr PB, Perlman S, 2021. COVID-19 treatments and pathogenesis including anosmia in K18-hACE2 mice. Nature 589:603-607. doi: 10.1038/s41586-020-2943-z.